Proceedings of the 11th World Congress on Electrical Engineering and Computer Systems and Sciences (EECSS'25)
Barcelona, Spain – August 19 - 21, 2024
Paper No. ICBES 118
DOI: 10.11159/icbes25.118

Monte Carlo Simulation and Optofluidic Techniques for Detecting Enterococcus Faecalis and Enterococcus Faecium

Quoc-Thinh Dinh[1], Hsin-Yu Chuang[1], Dang Khoa Tong[2], Wen-Chien Chuang[1], Cheng-Yen Kao[2]
Cheng-Yang Liu[1,*]
[1]Department of Biomedical Engineering
National Yang Ming Chiao Tung University, Taipei, Taiwan
dinhthinh0507.be12@nycu.edu.tw; melookuki4327.be12@nycu.edu.tw; yuki1357913@gmail.com; cyliu66@nycu.edu.tw
[2]Institute of Microbiology and Immunology
National Yang Ming Chiao Tung University, Taipei, Taiwan
tongkhoa40@gmail.com; kaocy@nycu.edu.tw

Abstract **-** This study presents a novel optofluidic system enhanced with Monte Carlo simulations for the optical characterization of bacterial suspensions, focusing on *Enterococcus faecalis* and *Enterococcus faecium*. The integration of optofluidics and advanced simulation techniques enables precise measurements of optical properties, including scattering, absorption, transmission, and refractive index (R.I.), which are critical for microbial detection. The system demonstrated the ability to distinguish between the two bacterial species, with R.I. values ranging from 1.405–1.410 for *E. faecalis* and 1.395–1.400 for *E. faecium*. Experimental results showed consistent trends of reduced light transmission with increasing bacterial concentrations (125–500 ppm) and extended optical path lengths (6–18 mm). Monte Carlo simulations validated the findings with error margins below 5%, highlighting the robustness of this approach. This method provides a scalable solution for bacterial diagnostics in clinical and environmental applications by achieving accurate, reproducible results and offering unique refractive index determination capabilities.

Keywords**:** Optofluidics, Monte Carlo simulations, Refractive index, *Enterococcus faecalis*, *Enterococcus faecium*, Optical characterization, Microfluidic diagnostics.

1. Introduction

Optofluidics, integrating optical and microfluidic technologies, has demonstrated significant potential in biological sample detection but faces challenges such as weak signals and fabrication limitations [1]–[4]. Kebabian's optical extinction monitor, utilizing cavity-enhanced detection, achieved sub-percent accuracy for detecting small biomolecules [5]. Eneren's work on light extinction spectroscopy showed sensitivity to refractive index variations with uncertainties under 2%, enabling reliable biological applications [6]. Chartier and Greenslade improved weak signal detection with a multi-pass extinction spectrometer, increasing the signal-to-noise ratio by 20% [7]. These advances underscore optofluidics' ability to provide efficient solutions for biomolecular detection.

Monte Carlo simulations further address challenges like weak signals and complex light interactions by modeling light scattering, absorption, and transmission in biological samples. Barbosa et al. achieved 95% accuracy in predicting scattering patterns in dusty plasma environments [8]. Xiang reduced particle size measurement errors to less than 2% in flames [9], while Knysh improved optical sensitivity for biomedical nanoparticles, enabling precise refractive index detection [10]. These tools enhance optofluidic systems, offering robust, reliable results for biomolecular analysis.

Detecting *Enterococcus faecalis* (*E. faecalis*) and *Enterococcus faecium (E. faecium)* remains difficult due to their complex optical and biological properties. Traditional culture-based methods take 24–48 hours, unsuitable for bacterial loads exceeding 10^5 CFU/mL, while PCR offers 10 CFU/mL sensitivity but involves contamination risks and extensive preparation [11], [12]. Immunoassays with 10^3 CFU/mL limits face cross-reactivity issues, complicating differentiation [13]. Additionally, their biofilm formation and intracellular invasion enable them to evade conventional detection techniques. Systems like the BioFire FilmArray offer rapid results at 10 CFU/mL sensitivity but are expensive and require specialized equipment [15]. Integrating optofluidics and Monte Carlo simulations, optimizing light scattering, absorption, and transmission, provides a scalable, rapid, and sensitive detection approach.

This study combines optofluidic systems with Monte Carlo simulations to enhance the detection of *E. faecalis* and *E. faecium*, overcoming the limitations of traditional methods. Optofluidic systems offer precise handling of small biological samples, while Monte Carlo simulations reveal detailed light-bacteria interactions. Together, they enable fast, affordable, and accurate bacterial identification and measurement, addressing the inefficiencies of current detection techniques.

2. Principle and Experimental setup

2.1. Monte Carlo method

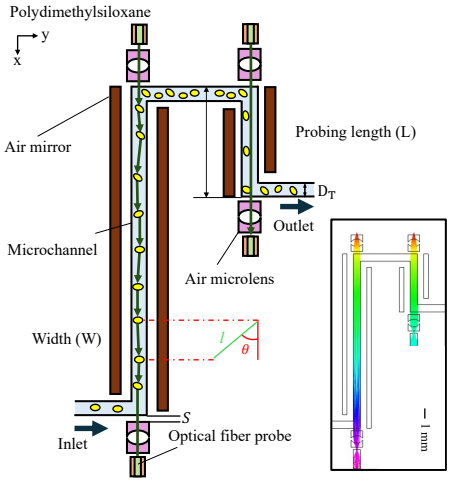

Fig. 1: Schematic of the lab-on-a-chip system with three microchannels (6 mm, 12 mm, 18 mm) for photon analysis.

The Monte Carlo method is a computational framework used to simulate light extinction by tracking individual photon interactions, such as scattering, absorption, and transmission, in a medium containing uniform particles. Figure 1 illustrates the optical microfluidic system used for this purpose, highlighting the size parameters implemented in the Monte Carlo simulations within the microfluidic system. Each photon begins with an initial position, randomly distributed across the source width to mimic realistic light distribution. The initial coordinates of the photon are defined as:

$$\begin{cases} x_0 = 0 \\ y_0 = (\varepsilon_1 - 0.5) D_T \end{cases} \tag{1}$$

where x_0, y_0 are the photon's starting coordinates; D_T is the width of the light source; ε_1 is a random number uniformly distributed in $[0,1]$, ensuring photons are evenly distributed along the source.

The photon travels a random distance l before interacting with a particle. This distance is calculated using:

$$l = -\frac{\ln \varepsilon_2}{\tau} \tag{2}$$

where ε_2 is a random number following a uniform distribution in the interval [0, 1]; τ is the tturbidity of the medium. Photon interactions are categorized as absorption, scattering, transmission, or escape. The outcomes are determined probabilistically:

$$\begin{cases} (\varepsilon_3 > \alpha) \cup (n \geq 1): \textit{Absorbed} \\ (x > S + L) \cup (n < 1): \textit{Transmitted} \\ (S < x < S + L) \cup \left(y < \left|\frac{W}{2}\right|\right): \textit{Scattered} \\ \textit{Others: escape} \end{cases} \tag{3}$$

where, $\alpha = C_{sca} / C_{ext}$ is the albedo, representing the proportion of extinction due to scattering. In this case, the photon is removed from the simulation, contributing to the absorption measurement.

In the case of multiple scattering, the spatial angle distribution following photon-particle collision can be determined using the Henyey-Greenstein phase function [19], expressed as the scattering angle:

$$\theta_0 = arcos\left\{\frac{1}{2g}\left[1 + g^2 - \left(\frac{1-g^2}{1-g+2g\varepsilon_3}\right)^2\right]\right\} \tag{4}$$

where g is the asymmetry factor.

After an interaction, the photon's new position is calculated iteratively based on its path length and scattering angle:

$$\begin{cases} x_{n+1} = x_n + l/\ cos\theta_n \\ y_{n+1} = y_n + l/\ sin\theta_n \end{cases} \tag{5}$$

where x_n, y_n are the current coordinates of the photon, θ_n: Scattering angle from the Henyey-Greenstein phase function. This iterative update ensures that photon trajectories are accurately tracked through the medium.

In Monte Carlo simulations, the transmittance T_{sim} measures the fraction of photons that pass through a medium without being absorbed or scattered. It is calculated as:

$$T_{sim} = \frac{\text{Transmitted Photons}}{\text{Total Emitted Photons}} = \frac{N}{N_0} \tag{5}$$

Here, N is the number of photons successfully transmitted through the medium, and N_0 is the total number of photons emitted by the source. This relationship provides a straightforward way to assess the transparency of the medium. From T_{sim}, the extinction coefficient $\tau = -\ln(T_{sim})$.This calculation connects photon interactions to measurable properties, allowing for the analysis of light scattering, absorption, and overall medium turbidity simply and intuitively.

2.2. Equipment and Bacteria Preparation

The fabrication process and experimental setup, shown in Figure 2, were carefully designed. In the design phase, microfluidic chip structures were modeled using 3D software to ensure precise dimensions. Mold fabrication was performed with a CNC milling machine (MDX-50, Roland, Japan) to create high-accuracy PMMA molds. Liquid PDMS (Polydimethylsiloxane) was poured into these molds, cured, and peeled off to preserve microchannel integrity. Oxygen plasma treatment (Piezobrush PZ3, Relyon Plasma, Germany) enhanced bonding between PDMS and glass substrates, ensuring structural stability. Dimensional verification was conducted using a Laser Microscope (VK-X3000, Keyence, Japan). During optical experiments, a Halogen Light Source (L-H100, Nikon, Japan) provided illumination, and a spectrometer (HRS-BD1-025, Princeton Instruments, USA) captured light transmission spectra. A peristaltic pump (MP-3000, Masterflex, USA) regulated fluid flow, while optical fiber probes (SIH200 37A, Thorlabs, USA) transmitted and collected light. This systematic process enabled precise characterization of bacterial suspensions in the lab-on-a-chip system.

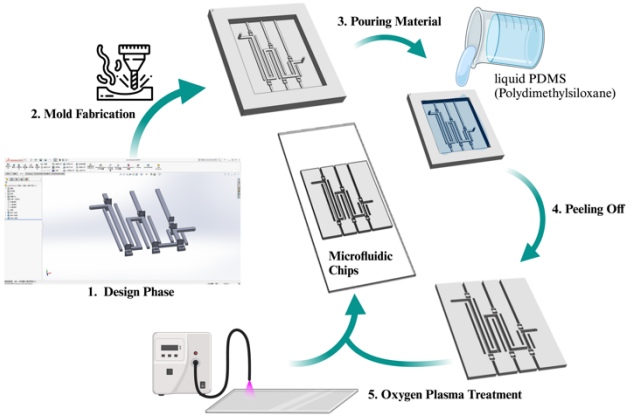

Fig. 2: Fabrication Workflow for Microfluidic Chip Development.

The system features three microchannels with optical path lengths of 6 mm, 12 mm, and 18 mm, designed for studying bacteria suspensions. Each channel, 750 µm wide and 470 µm deep, ensures smooth fluid flow and precise measurements. Air microlenses focus incoming light, and air mirrors reflect it along the path to enhance interactions with the bacterial sample. Scattered photons change direction, absorbed photons lose energy, and penetrated photons pass through unaffected. The probing length is the region where these interactions are analyzed using the Monte Carlo method. Optical fiber probes guide light at the inlet and outlet, enabling accurate analysis of bacterial concentration, size, and optical properties, as shown in Figure 3.

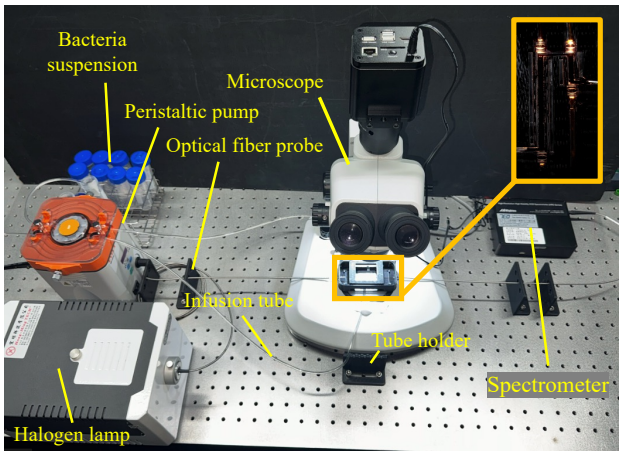

Fig. 3: Experimental setup showing the halogen lamp, peristaltic pump, optical fiber probe, spectrometer, and E. *faecalis* and E. *faecium* suspension. Inset: microfluidic chip.

This study focused on clinical isolates of E. *faecalis* and E. *faecium*, two significant bacterial pathogens. Strains were stored at −80 °C in Luria-Bertani (LB) medium with 20% glycerol to maintain viability. Before experimentation, the isolates were revived on LB agar or tryptic soy agar (TSA) and incubated at 37 °C for 18 hours to ensure uniform growth. Overnight cultures were then prepared by inoculating single colonies into sterile LB medium and incubating at 37 °C with shaking at 200 rpm for 16–18 hours, producing dense bacterial cultures in the exponential phase. Following incubation, cultures were centrifuged at 4700 rpm for 10 minutes to pellet the cells, which were then resuspended in 0.9% sodium chloride (NaCl) to standardize the bacterial suspension. Optical density at 600 nm (OD600) was measured, and bacterial concentrations were adjusted based on a standard curve to achieve the desired CFU/mL levels. This careful preparation ensured consistency and accuracy in downstream analyses, such as antimicrobial susceptibility tests and molecular assays targeting *E. faecalis* and *E. faecium*.

3. Results

3.1. Photon Behaviour Analysis

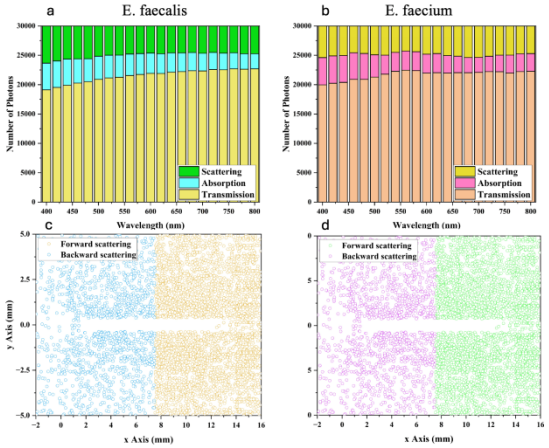

Fig. 4: Photon Interaction and Scattering Profiles for *E. faecalis* and *E. faecium*: (a) Photon interactions (scattering, absorption, and transmission) for E. faecalis across wavelengths; (b) Photon interactions for *E. faecium* across wavelengths; (c) Forward and backward scattering patterns for *E. faecalis*; (d) Forward and backward scattering patterns for *E. faecium.*

Figure 4a and 4b depict photon events, scattering, absorption, and transmission, for *E. faecalis* and *E. faecium* across wavelengths. *E. faecalis* exhibits dominant scattering at 400–500 nm (>40%) and higher transmission (70%) at 800 nm, with low absorption throughout. *E. faecium* shows higher transmission at 800 nm (>75%) and reduced scattering at shorter wavelengths. These variations highlight the optical differences between the species, emphasizing the role of wavelength optimization for detection. Figures 4c and 4d detail scattering profiles, showing forward scattering as predominant for both bacteria, contributing 80% for *E. faecalis* and ~78% for *E. faecium*. Unique backward scattering patterns further enable species-specific detection, enhancing diagnostic accuracy.

3.2. Wavelength-Dependent Scattering and Absorption

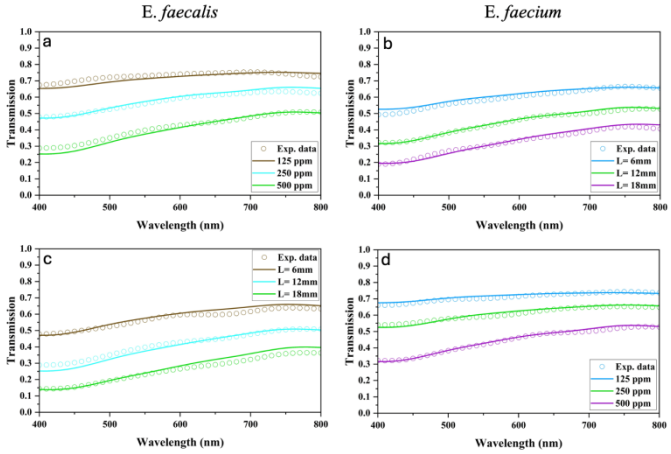

Fig. 5: Photon Interaction and Scattering Profiles for *E. faecalis* and *E. faecium*: (a) Photon interactions (scattering, absorption, and transmission) for *E. faecalis* across wavelengths; (b) Photon interactions for *E. faecium* across wavelengths; (c) Forward and backward scattering patterns for E. faecalis; (d) Forward and backward scattering patterns for E. faecium.

The transmission spectra in Figure 5 reveal differences in the optical behaviors of *E. faecalis* and *E. faecium* at varying concentrations and path lengths. Panels (a) and (b) show reduced light transmission from 125 ppm to 500 ppm, with *E. faecalis* showing stronger effects, likely due to its unique size, shape, or scattering properties. Harrison

demonstrated that spectral extinction techniques effectively analyze fluids with particles from nanometers to microns [16], while Duffy highlighted the benefits of microfluidic platforms for isolating and analyzing particles [17]. Panels (c) and (d) show increased attenuation at longer path lengths (6 mm to 18 mm) due to extended light interaction. Tang optimized microchannel designs for higher optical efficiency, and Caruso improved flow control for enhanced reproducibility [18, 19]. Mortelmans achieved 95% accuracy in detecting bacterial concentrations as low as 50 CFU/mL with optimized optical paths [20]. Monte Carlo simulations aligned closely with experimental data, validating their ability to predict light behaviors. Shaw achieved scattering predictions with less than 1.5% deviation, while Hartensveld improved detection sensitivity by 20% in noisy environments [21, 22].

3.3. Refractive index

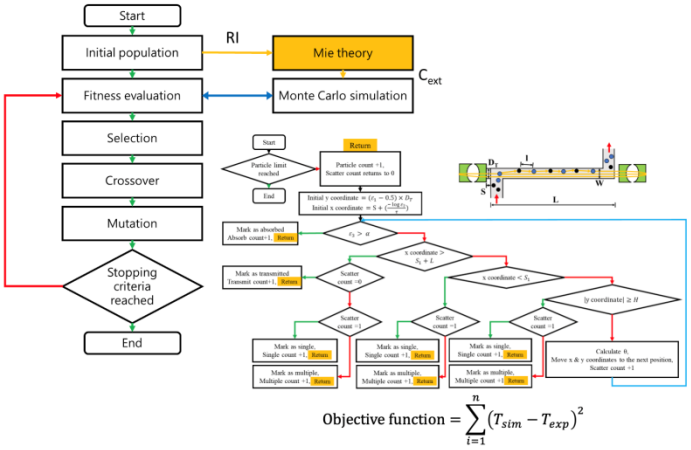

Fig. 6: Genetic algorithm flowchart integrated with Monte Carlo simulations for refractive index estimation.

Figure 6 illustrates the framework combining the genetic algorithm (GA) with Monte Carlo simulations to estimate the refractive index (n) of bacterial suspensions, leveraging their scattering and extinction properties. The GA optimizes refractive index values through iterative processes of fitness evaluation, selection, crossover, and mutation. Monte Carlo simulations integrate Mie theory to calculate the extinction cross-section C_{ext} based on photon interactions, feeding back into the GA for precise adjustments. The decision-making process embedded within the framework ensures accurate modeling of light behaviour, such as scattering and absorption. This hybrid approach yields highly accurate predictions of optical properties with minimal error.

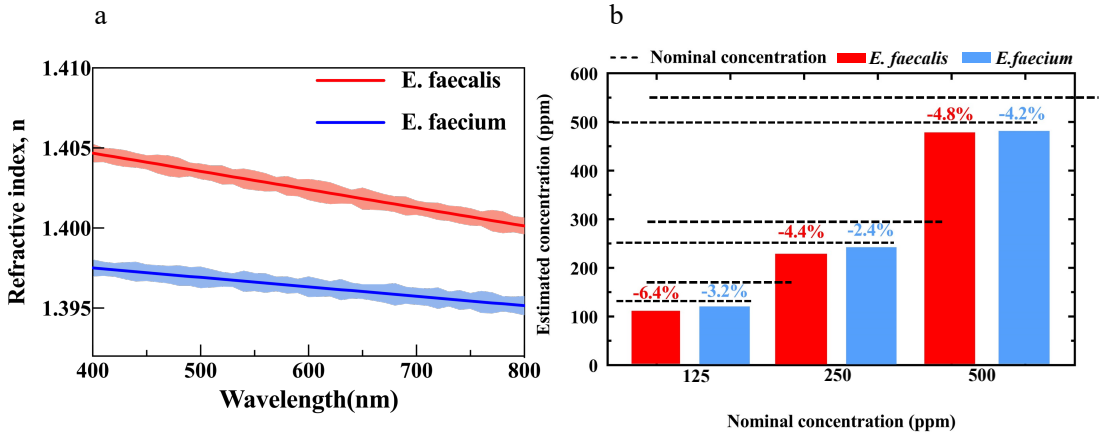

Fig. 7: (a) Refractive indices of *E. faecalis* and *E. faecium* decrease with wavelength. (b) Estimated concentrations closely match nominal values

Figure 7 illustrates the refractive indices of *E. faecalis* and *E. faecium* across the visible spectrum (400–800 nm). Both species show a gradual decline in as the wavelength increases, consistent with trends in biological suspensions. The mean values for *E. faecalis* range from 1.405 to 1.402, while those for *E. faecium* are slightly lower, ranging from 1.399 to 1.396. These findings are supported by Shaw et al., who emphasized the role of microfluidic platforms in achieving precise optical measurements [22]. Mortelmans et al. further demonstrated that optimizing optical path lengths enhances the sensitivity and reproducibility of refractive index measurements for bacterial suspensions [19]. The concentration estimation results for *E. faecalis* and *E. faecium*, presented in Figure 7b, highlight the accuracy of the optofluidic and Monte Carlo-based methodology. Deviations for *E. faecalis* reach up to 6.4% at 125 ppm but decrease at higher concentrations, with 4.8% at 500 ppm. Conversely, *E. faecium* shows more consistent accuracy, with deviations between 2.4% and 4.2%. The higher errors for *E. faecalis* at lower concentrations may stem from its stronger scattering effects and greater sensitivity to path length variations.

4. Conclusion

In conclusion, this study demonstrates the unique capability of the optofluidic system integrated with Monte Carlo simulations to accurately characterize bacterial suspensions, particularly *E. faecalis* and *E. faecium*. The approach effectively measures optical transmission, scattering, and the R.I. values ranging from 1.405 to 1.410 for *E. faecalis* and 1.395 to 1.400 for *E. faecium*. Transmission behavior was highly dependent on bacterial concentration and optical path length, with longer paths (6 mm to 18 mm) resulting in increased attenuation. Monte Carlo simulations validated experimental results with errors under 5%, highlighting their precision in modeling light-particle interactions. Furthermore, the system demonstrated sensitivity to bacterial concentrations, with nominal vs. estimated errors as low as -2.4%. This capability to determine the refractive index uniquely positions the proposed methodology as a scalable and reliable tool for microbial diagnostics in clinical and environmental applications.

Acknowledgements

This work is supported by National Science and Technology Council of Taiwan (113-2221-E-A49-071, 113-2223-E-007-005, 114-2221-E-A49-064-MY3).

References

[1] P. L. Kebabian, W. A. Robinson, and A. Freedman, “Optical extinction monitor using cw cavity enhanced detection,” *Review of Scientific Instruments*, vol. 78, no. 6, 2007.

[2] P. Eneren, Y. T. Aksoy, Y. Zhu, E. Koos, and M. R. Vetrano, “Light extinction spectroscopy applied to polystyrene colloids: Sensitivity to complex refractive index uncertainties and to noise,” *Journal of Quantitative Spectroscopy and Radiative Transfer*, vol. 261, p. 107494, 2021.

[3] R. Chartier and M. E. Greenslade, “Initial investigation of the wavelength dependence of optical properties measured with a new multi-pass Aerosol Extinction Differential Optical Absorption Spectrometer (AE-DOAS),” *Atmospheric Measurement Techniques*, vol. 5, no. 4, pp. 709–721, 2012.

[4] S. Barbosa, F. R. Onofri, L. Couëdel, M. Wozniak, C. Montet, C. Pelcé, C. Arnas, L. Boufendi, E. Kovacevic, and J. Berndt, “An introduction to light extinction spectrometry as a diagnostic for dust particle characterisation in dusty plasmas,” *Journal of Plasma Physics*, vol. 82, no. 4, p. 615820403, 2016.

[5] H. Xiang, B. Cheng, C. Zhang, and W. Qiao, “Study of particle size measurement by the extinction method in flame,” *Energies*, vol. 16, no. 12, p. 4792, 2023.

[6] A. Knysh, P. Sokolov, and I. Nabiev, “Dynamic Light Scattering Analysis in Biomedical Research and Applications of Nanoparticles and Polymers,” *Journal of Biomedical Photonics & Engineering*, vol. 9, no. 2, p. 020203, 2023.

[7] S. Gordon, R. Hammond, K. Roberts, N. Savelli, and D. Wilkinson, “In-process particle characterization by spectral extinction,” *Chemical Engineering Research and Design*, vol. 78, no. 8, pp. 1147–1152, 2000.

[8] P. A. Ryan, “Improved light extinction reconstruction in interagency monitoring of protected visual environments,” *Journal of the Air & Waste Management Association*, vol. 55, no. 11, pp. 1751–1759, 2005.

[9] R. Rahmatullah and S. Suparno, “The Development of Experimental Absorption Based on Arduino-Uno and Labview on Light Radiation by Colourful Surface,” *Jurnal Pendidikan Fisika Indonesia*, vol. 16, no. 1, pp. 41–46, 2020.

[10] M. P. Miranda-Hernández, E. R. Valle-González, D. Ferreira-Gómez, N. O. Pérez, L. F. Flores-Ortiz, and E. Medina-Rivero, "Theoretical approximations and experimental extinction coefficients of biopharmaceuticals," *Analytical and Bioanalytical Chemistry*, vol. 408, no. 5, pp. 1523–1530, 2016.
[11] W. Hongjun, W. Chen, L. Bingcai, and T. Ailing, "Research on Rapid Measurement Technology of Roughness Based on Light Scattering," in *Journal of Physics: Conference Series*, IOP Publishing, 2022.
[12] W. Hergert, "Gustav Mie: From electromagnetic scattering to an electromagnetic view of matter," in *The Mie Theory: Basics and Applications*, Springer, 2012, pp. 1–51.
[13] N. J. Shetty, A. Pandey, S. Baker, W. M. Hao, and R. K. Chakrabarty, "Measuring light absorption by freshly emitted organic aerosols: optical artifacts in traditional solvent-extraction-based methods," *Atmospheric Chemistry and Physics*, vol. 19, no. 13, pp. 8817–8830, 2019.
[14] D. C. Duffy, J. C. McDonald, O. J. Schueller, and G. M. Whitesides, "Rapid prototyping of microfluidic systems in poly(dimethylsiloxane)," *Analytical Chemistry*, vol. 70, no. 23, pp. 4974–4984, 1998.
[15] P. A. Ryan, D. Lowenthal, and N. Kumar, "Precipitation in light extinction reconstruction," *Journal of the Air & Waste Management Association*, vol. 55, no. 7, pp. 1014–1018, 2005.
[16] D. J. Harrison, A. Manz, Z. Fan, H. M. Lüdi, and H. M. Widmer, "Capillary electrophoresis and sample injection systems integrated on a planar glass chip," *Analytical Chemistry*, vol. 64, no. 17, pp. 1926–1932, 1992.
[17] S. Tang and G. M. Whitesides, "Basic microfluidic and soft lithographic techniques," *Advanced Materials*, vol. 21, no. 34, pp. 3507–3530, 2009.
[18] G. Caruso, "Microfluidics and mass spectrometry in drug discovery and development: from synthesis to evaluation," *Frontiers in Pharmacology*, vol. 14, p. 1201926, 2023.
[19] T. Mortelmans, D. Kazazis, J. Werder, P. M. Kristiansen, and Y. Ekinci, "Injection molding of thermoplastics for low-cost nanofluidic devices," *ACS Applied Nano Materials*, vol. 5, no. 12, pp. 17758–17766, 2022.
[20] J. M. Shaw, J. D. Gelorme, N. C. LaBianca, W. E. Conley, and S. J. Holmes, "Negative photoresists for optical lithography," *IBM Journal of Research and Development*, vol. 41, no. 1.2, pp. 81–94, 1997.
[21] M. Hartensveld, "Optimization of dry and wet GaN etching to form high aspect ratio nanowires," *Rochester Institute of Technology*, 2018.
[22] R. Rahman, S. Hossain, and T. Chakraborty, "Advancements in biosensing using microfluidics: Application in medical diagnostics," *Sensors and Actuators B: Chemical*, vol. 245, pp. 588–604, 2022.